

recording of the ^{197}Au Mössbauer spectra. The investigations were partly supported by the Netherlands Foundation for Chemical Research (SON), with financial aid from the Netherlands Organization for the Advancement of Pure Research (ZWO).

Registry No. $[\text{Au}_7\text{L}_7](\text{OH})$, 88056-72-8; $[\text{Au}_9\text{L}_8](\text{NO}_3)_3$,

37336-35-9.

Supplementary Material Available: Tables of structure factors, positional parameters of the phenyl carbon atoms and the residual peaks between the clusters, distances of the Au and P atoms to the least-squares planes defined by the equatorial gold atoms for all four gold $[\text{Au}_7\text{P}_7]^+$ cations, and anisotropic thermal parameters (59 pages). Ordering information is given on any current masthead page.

Contribution from the Department of Chemistry, Gorlaeus Laboratories, State University Leiden, Leiden, The Netherlands

Synthesis, Structure, and Magnetic Properties of Fluoride-Bridged Copper(II) Dimers. Crystal and Molecular Structures of Bis(μ -fluoro)bis[tris(3,4,5-trimethylpyrazole- N^2)copper(II)] Bis(tetrafluoroborate) and Bis(μ -fluoro)bis[(5-methylpyrazole- N^2)]bis(3,5-dimethylpyrazole- N^2)copper(II)] Bis(tetrafluoroborate)

FREDERIK J. RIETMEIJER, RUDOLF A. G. DE GRAAFF, and JAN REEDIJK*

Received April 7, 1983

The molecular structures of the compounds $[\text{Cu}_2\text{F}_2(\text{tmpz})_6](\text{BF}_4)_2$ and $[\text{Cu}_2\text{F}_2(\text{dmpz})_4(\text{mpz})_2](\text{BF}_4)_2$ (abbreviated as I and II, respectively, with tmpz = 3,4,5-trimethylpyrazole, dmpz = 3,5-dimethylpyrazole, and mpz = 5(3)-methylpyrazole), as determined by single-crystal X-ray analyses, are described. I was prepared from copper(II) tetrafluoroborate and tmpz. II was synthesized via partial substitution of dmpz ligands in $[\text{Cu}_2\text{F}_2(\text{dmpz})_6](\text{BF}_4)_2$. I crystallizes in the monoclinic space group $P2_1/n$ with two formula units in a cell of dimensions $a = 11.514(4) \text{ \AA}$, $b = 16.439(3) \text{ \AA}$, $c = 13.159(3) \text{ \AA}$, and $\beta = 101.82(2)^\circ$. II crystallizes in the monoclinic space group $P2_1/c$ with $a = 9.954(1) \text{ \AA}$, $b = 11.862(2) \text{ \AA}$, $c = 17.679(4) \text{ \AA}$, $\beta = 99.45(1)^\circ$, and $Z = 2$. Reflection data were collected with an Enraf-Nonius CAD-4 single-crystal diffractometer and graphite-monochromatized Mo K α radiation. Both structures were solved with use of conventional Patterson, Fourier, and least-squares refinement techniques. The final R factors were $R = 0.033$ and $R_w = 0.04$ for I (based on 2553 independent reflections) and $R = 0.035$ and $R_w = 0.047$ for II (based on 2258 independent reflections). The compounds are dimeric, with asymmetric difluoro bridges between the copper ions (in I, the two Cu-F distances are 1.911(2) and 2.183(2) \AA; in II, they are 1.901(2) and 2.195(2) \AA, respectively). In I, the Cu-F-Cu angle ($94.59(7)^\circ$) is slightly larger than in II ($93.73(8)^\circ$), as is the case for the Cu-Cu distances (in I, Cu-Cu = 3.0141(8) \AA; in II, Cu-Cu = 2.9962(9) \AA). In both compounds the coordination geometry is approximately square-based pyramidal. The fluoride ion with the largest distance to copper forms the apical ligand. The structures are compared with closely related structures of copper(II) dimers. The observed ligand field spectra are in agreement with square-pyramidal coordination geometry. Magnetic susceptibility measurements down to 2 K are indicative of a very small exchange interaction ($|J| < 0.5 \text{ cm}^{-1}$). The EPR spectra are typical of Cu(II) dimers, showing both $\Delta m_s = 1$ and $\Delta m_s = 2$ transitions at various temperatures.

Introduction

In the last decade the increasing interest in magnetic exchange between paramagnetic transition-metal ions has stimulated the study of dimeric, cluster, and linear-chain compounds. A detailed investigation of the magnetic interaction is easier in well-defined structures containing isolated magnetic units. Also favorable is the presence of simple bridging ligands such as OH^- , F^- , Cl^- , Br^- , oxamido(2-), oxamato(2-), acetato(1-), etc. The fluoride-bridged compounds are less well-known because of their inaccessibility. Since the introduction of BF_4^- salt decomposition for the synthesis of fluoride-bridged transition-metal compounds, however, explorative work has resulted in a number of new compounds.¹⁻⁷ In this respect, the ligand-exchange method developed by Ten Hoedt, which involves the exchange of non-bridging ligands with other ligands, is of special interest.⁶ We now report the crystal and molecular structures of the copper(II) dimers

Table I. Crystal Data for I

$\text{Cu}_2\text{C}_{36}\text{H}_{60}\text{N}_{12}\text{B}_2\text{F}_{10}$	$V = 2438 \text{ \AA}^3$
mol wt 999.6	$Z = 2$
monoclinic, space group $P2_1/n$	$d_{\text{calcd}} = 1.361 \text{ g cm}^{-3}$
$a = 11.514(4) \text{ \AA}$	$d_{\text{obsd}}^a = 1.34(2) \text{ g cm}^{-3}$
$b = 16.439(3) \text{ \AA}$	$\mu(\text{Mo K}\alpha) = 10.1 \text{ cm}^{-1}$
$c = 13.159(3) \text{ \AA}$	cryst dims
$\beta = 101.82(2)^\circ$	$0.40 \times 0.35 \times 0.20 \text{ mm}$

^a By the flotation method ($\text{CHCl}_3/\text{C}_2\text{H}_5\text{OH}$).

Table II. Crystal Data for II

$\text{Cu}_2\text{C}_{28}\text{H}_{44}\text{N}_{12}\text{B}_2\text{F}_{10}$	$V = 2059 \text{ \AA}^3$
mol wt 887.6	$Z = 2$
monoclinic, space group $P2_1/c$	$d_{\text{calcd}} = 1.431 \text{ g cm}^{-3}$
$a = 9.954(1) \text{ \AA}$	$d_{\text{obsd}}^a = 1.43(2) \text{ g cm}^{-3}$
$b = 11.862(2) \text{ \AA}$	$\mu(\text{Mo K}\alpha) = 11.1 \text{ cm}^{-1}$
$c = 17.679(4) \text{ \AA}$	cryst dims
$\beta = 99.45(1)^\circ$	$0.25 \times 0.25 \times 0.50 \text{ mm}$

^a By the flotation method ($\text{CHCl}_3/\text{C}_2\text{H}_5\text{OH}$).

$[\text{Cu}_2\text{F}_2(\text{tmpz})_6](\text{BF}_4)_2$ (I) and $[\text{Cu}_2\text{F}_2(\text{dmpz})_4(\text{mpz})_2](\text{BF}_4)_2$ (II) together with spectroscopic and magnetic data. The results are compared with those of previous studies on related compounds.

Experimental Section

Syntheses. Commercial $\text{Cu}(\text{BF}_4)_2 \cdot 6\text{H}_2\text{O}$ and 3(5)-methylpyrazole (mpz, Aldrich) were used without further purification. 3,4,5-Tri-methylpyrazole (tmpz) was prepared by a method described by

- Guichelaar, M. A.; Van Hest, J. A. M.; Reedijk, J. *Inorg. Nucl. Chem. Lett.* **1974**, *10*, 999-1004.
- Reedijk, J.; Jansen, J. C.; Van Koningsveld, H.; Van Kralingen, C. G. *Inorg. Chem.* **1978**, *17*, 1990-1994.
- Verbiest, J.; Van Ooijen, J. A. C.; Reedijk, J. *J. Inorg. Nucl. Chem.* **1980**, *42*, 971-975.
- Ten Hoedt, R. W. M.; Reedijk, J. *Inorg. Chim. Acta* **1981**, *51*, 23-27.
- Ten Hoedt, R. W. M.; Reedijk, J.; Verschoor, G. C. *Recl. Trav. Chim. Pays-Bas* **1981**, *100*, 400-405.
- Reedijk, J.; Ten Hoedt, R. W. M. *Recl. Trav. Chim. Pays-Bas* **1982**, *101*, 49-57.
- Reedijk, J. *Comments Inorg. Chem.* **1982**, *1* (6), 379-389.

Rabjohn.⁸ $[\text{Cu}_2\text{F}_2(\text{dmpz})_6](\text{BF}_4)_2$ was prepared according to Ten Hoedt.⁵

I was prepared by mixing $\text{Cu}(\text{BF}_4)_2 \cdot 6\text{H}_2\text{O}$ (0.70 g, 2.0 mmol) with tmpz (1.10 g, 10 mmol) in ethanol (15 mL). A light blue crystalline material separated. The solid was collected by filtration, washed with ether, and dried in vacuo. II was synthesized with use of the ligand-exchange method mentioned above. The procedure is analogous to the one reported in the literature⁵ for the synthesis of $[\text{Cu}_2\text{F}_2(\text{mpz})_4(\text{dmpz})_2](\text{BF}_4)_2$; however, lower concentrations were used throughout this synthesis. $[\text{Cu}_2\text{F}_2(\text{dmpz})_6](\text{BF}_4)_2$ (1.00 g, 1.1 mmol) and 3-methylpyrazole (0.90 g, 11 mmol) were refluxed in ethanol (90 mL) for 30 min. The solution was filtered while hot; when the filtrate cooled to room temperature blue crystals separated. The product was collected by filtration, washed with ethanol and diethyl ether, and dried in vacuo. I and II gave satisfactory elemental analyses. (Anal. Found (Calcd for I, $\text{Cu}_2\text{C}_{36}\text{H}_{60}\text{N}_{12}\text{B}_2\text{F}_{10}$): Cu, 12.27 (12.71); C, 42.41 (43.25); H, 6.00 (6.05); N, 17.08 (16.81); F, 19.2 (19.01). Found (Calcd for II, $\text{Cu}_2\text{C}_{28}\text{H}_{44}\text{N}_{12}\text{B}_2\text{F}_{10}$): Cu, 14.16 (14.32); C, 37.88 (37.90); H, 5.01 (5.00); N, 18.9 (18.94); F, 21.1 (21.41)). Crystal data are given in Tables I and II, respectively.

Analyses and Physical Measurements. Carbon, hydrogen, nitrogen, and fluorine analyses were performed by Dr. Pascher, Bonn, West Germany. Metal analyses were carried out with use of standard EDTA-titration techniques. Infrared spectra ($4000\text{--}180\text{ cm}^{-1}$) were recorded on a Perkin-Elmer 580 spectrophotometer. Ligand field spectra were recorded on a Beckman DK-2A reflectance spectrophotometer (reference MgO). EPR powder spectra were recorded on commercial Varian instruments at X-band and at Q-band frequencies at several temperatures. Magnetic susceptibility measurements down to 2 K were carried out on solid polycrystalline samples with a parallel-field vibrating-sample magnetometer (PAR Model 150A).

X-ray Data Collection and Structure Determination. I. A crystal of dimensions $0.40 \times 0.35 \times 0.20\text{ mm}$ was sealed in a thin-walled glass capillary tube and mounted on a Nonius CAD-4 diffractometer. Room-temperature diffractometer data and Weissenberg photographs were indicative of the monoclinic space group $P2_1/n$. Precise lattice constants were determined by least-squares refinement of the angular settings of 24 reflections. Crystal data are listed in Table I. Intensities were collected in the ω - θ scan mode for all reflections with $2^\circ < \theta < 23^\circ$ and with $k > 0$, with use of graphite-monochromatized $\text{Mo K}\alpha$ radiation. The scanning rate was adjusted to the required precision of $\sigma(I) < 0.01I$, with a maximum scan time of 90 s/reflection. Intensities I and their estimated standard deviations (hereafter esd's) were calculated from counting statistics. Three standard reflections were measured after every 5400 s of radiation time to check for instrumental instability and crystal decomposition; during the data collection there was an 8% decrease in intensity, for which the data were corrected. The maximal variation of 6% in the intensity of a suitable reflection at different azimuthal positions and the value of μ suggested that no absorption correction was necessary. The intensities of 5392 reflections were measured, 3373 of which were symmetry independent. A total of 2553 reflections with $I > 2\sigma(I)$ were considered significant. The measured intensities were corrected for Lorentz and polarization effects. The calculations were performed on the Leiden University Amdahl V7B computer, using a local set of computer programs. Scattering factors for neutral atoms have been taken from ref 9 and where appropriate used with correction for the anomalous scattering. The structure was solved with use of the heavy-atom method and refined by blocked-matrix least-squares calculations, except for the first few cycles of refinement, when isotropic thermal parameters were used, and the last cycle, when a full matrix was used. The initial stages were carried out with unit weights; in the final cycles, however, weights $1/\sigma^2(F)$ were used (with $\sigma(F) = \sigma(F)$ counting statistics + $0.03F$). Wherever possible, hydrogen atom positions were obtained from difference Fourier syntheses, otherwise calculated positions were used. Although the positional and isotropic thermal parameters of the methyl group protons became rather large, the C-H bond lengths remained realistic. Group refinement of the BF_4^- ion was used in the early stages of refinement. A model, consisting of two tetrahedra with a common center, was refined initially

Table III. Final Fractional Coordinates ($\times 10^4$) of Non-Hydrogen Atoms in I, with Esd's in Parentheses

atom	<i>x/a</i>	<i>y/b</i>	<i>z/c</i>
Cu	138.4 (4)	389.2 (2)	3994.7 (3)
F	495 (2)	-752 (1)	4851 (2)
N(11)	1430 (3)	1726 (2)	5141 (3)
N(12)	1592 (3)	1035 (2)	4626 (2)
C(13)	2755 (3)	934 (2)	4831 (2)
C(14)	3328 (3)	1548 (2)	5464 (3)
C(15)	2449 (4)	2043 (2)	5647 (3)
C(16)	3308 (5)	212 (4)	4438 (6)
C(17)	4630 (5)	1649 (5)	5897 (6)
C(18)	2469 (8)	2785 (4)	6311 (6)
N(21)	-2302 (3)	889 (2)	3462 (3)
N(22)	-1555 (3)	316 (2)	3223 (2)
C(23)	-2232 (3)	-156 (2)	2515 (3)
C(24)	-3397 (4)	133 (3)	2317 (3)
C(25)	-3405 (3)	789 (3)	2940 (3)
C(26)	-1761 (6)	-884 (4)	2075 (5)
C(27)	-4437 (8)	-218 (9)	1553 (7)
C(28)	-4368 (6)	1354 (6)	3082 (6)
N(31)	1183 (3)	-872 (2)	2914 (2)
N(32)	835 (3)	-83 (2)	2884 (2)
C(33)	1100 (3)	217 (2)	2023 (3)
C(34)	1612 (3)	-374 (2)	1506 (2)
C(35)	1639 (3)	-1065 (2)	2093 (3)
C(36)	864 (6)	1090 (3)	1746 (5)
C(37)	2024 (7)	-283 (4)	502 (5)
C(38)	2106 (10)	-1908 (4)	1986 (6)
B	-1479 (6)	2676 (3)	5260 (5)
F(1A)	-1362 (3)	3537 (2)	5345 (2)
F(2A)	-652 (3)	2364 (1)	6080 (2)
F(3A)	-2541 (3)	2430 (2)	5379 (3)
F(4A)	-1406 (3)	2428 (2)	4294 (2)
F(1B)	-1866 (3)	3409 (2)	5440 (2)
F(2B)	-556 (3)	2416 (1)	6051 (2)
F(3B)	-2380 (3)	2079 (2)	5231 (3)
F(4B)	-1045 (3)	2602 (2)	4364 (2)

Table IV. Relevant Bond Lengths (Å) and Angles (deg) in I,^a with Esd's in Parentheses

Cu-Cu'	3.0141 (8)	Cu-N(12)	2.013 (3)
Cu-F	2.183 (2)	Cu-N(22)	2.009 (3)
Cu-F'	1.911 (2)	Cu-N(32)	1.965 (3)
Cu-F-Cu'	94.59 (7)	F-Cu-F'	85.41 (7)
N(12)-Cu-F	100.8 (1)	N(12)-Cu-F'	85.9 (1)
N(22)-Cu-F	105.7 (1)	N(22)-Cu-F'	86.1 (1)
N(32)-Cu-F	88.94 (9)	N(32)-Cu-F'	174.3 (1)
N(12)-Cu-N(22)	151.6 (1)	N(12)-Cu-N(32)	94.8 (1)
N(22)-Cu-N(32)			95.9 (1)

^a Primed atoms are generated by the center of symmetry.

with use of slack constraints¹⁰ ($\text{B-F} = 1.351\text{ \AA}$ with $\sigma = 0.002\text{ \AA}$, $\text{F-F} = 2.206\text{ \AA}$ with $\sigma = 0.002\text{ \AA}$). The thermal parameters of the atoms were fixed at 6 \AA^2 , and the occupancy ratio (1/1) of the two tetrahedra A and B was not refined. Subsequently, the positional and the isotropic thermal parameters of the corresponding atoms in the tetrahedra A and B were coupled, the geometrical constraints were removed, and the occupancy ratio of A and B was allowed to refine. Finally, a few cycles of anisotropic refinement of the complete model (including the BF_4^- ion) resulted in $R = \sum ||F_o| - |F_c|| / \sum |F_o| = 0.033$ and $R_w = [\sum w(|F_o| - |F_c|)^2 / \sum wF_o^2]^{1/2} = 0.043$ for the 2553 significant reflections. The occupancies of A and B were 27 and 73% ($\sigma = 1\%$), respectively. A final difference Fourier synthesis showed no significant residual peaks except for two small peaks in the vicinity of the BF_4^- atoms, probably due to the presence of a small percentage of other conformations than A and B alone. Final fractional coordinates of nonhydrogen atoms are listed in Table III, while Table IV summarizes the most relevant interatomic distances and angles. Hydrogen-bond information is given in Table V. Fractional coordinates of hydrogen atoms, additional interatomic distances and angles, and all thermal parameters are given in the supplementary material, together with

(8) Rabjohn, N. "Organic Syntheses"; Wiley: New York, 1963; Collect. Vol. IV.

(9) "International Tables of X-ray Crystallography"; Kynoch Press: Birmingham, England, 1974; Vol. 4.

(10) Waser, J. *Acta Crystallogr.* **1963**, *16*, 1091-1094.

Table V. Hydrogen-Bonding Distances (Å) and Angles (deg) in I,^a with Esd's in Parentheses

N(11)--F'	2.736 (4)	H(11)--F'	2.35 (5)
N(11)--F(2A)	3.096 (5)	H(11)--F(2A)	2.49 (4)
N(11)--F(2B)	3.012 (5)	H(11)--F(2B)	2.41 (4)
N(11)--F(4B)	3.170 (5)	H(11)--F(4B)	2.55 (4)
N(21)--F'	2.723 (4)	H(21)--F'	2.34 (5)
N(21)--F(3B)	3.056 (6)	H(21)--F(3B)	2.41 (4)
N(21)--F(4A)	2.864 (5)	H(21)--F(4A)	2.25 (5)
N(31)--F	2.826 (4)	H(31)--F	2.23 (4)
N(31)--F(2A)'	2.910 (4)	H(31)--F(2A)'	2.26 (4)
N(11)--H(11)--F'	118 (4)	N(21)--H(21)--F'	116 (4)
N(11)--H(11)--F(2A)	148 (5)	N(21)--H(21)--F(3B)	154 (5)
N(11)--H(11)--F(2B)	147 (5)	N(21)--H(21)--F(4A)	146 (5)
N(11)--H(11)--F(4B)	151 (5)	N(31)--H(31)--F	134 (4)
N(31)--H(31)--F(2A)'			142 (4)

^a Very weak hydrogen bonds are omitted. Primed atoms are generated by the symmetry operation $-x, -y, 1-z$.

least-squares planes and a list of observed and calculated structure factors.

II. The data collection procedure was analogous to the one reported above. Weissenberg photographs and diffractometer data suggested the space group $P2_1/c$. Crystal data are listed in Table II. Intensity data were collected in the ω - θ scan mode for all reflections with $2^\circ < \theta < 24^\circ$ and with $h > 0$ and $k > 0$ using graphite-monochromatized Mo K α radiation. During the data collection there was a 5% decrease in intensity for which the data were corrected. The data were not corrected for absorption: the intensity of a chosen reflection at different azimuthal positions varied no more than 5%, while the μ value was 11.1 cm⁻¹. The intensities of 3443 reflections were measured, 3235 of which were symmetry independent. A total of 2258 reflections with $I > 2\sigma(I)$ were considered significant. The refinement was carried out as described above, with the following exceptions: (i) the isotropic thermal parameters of the methyl hydrogens were fixed at a value of $B = 8 \text{ \AA}^2$; (ii) the BF₄⁻ anions was refined in one conformation only. During the initial stages of refinement there was some doubt about the kind of atom attached to carbon atom C(13), when the isotropic thermal parameter of the hydrogen atom at that place appeared to have a small negative value ($B = -1 \text{ \AA}^2$). Introduction of a carbon atom instead resulted in a large positive increase of this thermal parameter. Moreover, this carbon atom would then be at a 2.2-Å distance of its symmetry equivalent in a neighboring dimer, which is impossible. Therefore, it was concluded that the atomic position involved must be occupied partly by hydrogen and partly by carbon. In an attempt to explain this phenomenon two possibilities were taken into account: (1) the presence of two tautomeric methylpyrazole rings in the structure, one with the methyl group in the 3-position and one with the methyl group in the 5-position; (2) the presence of some Cu₂F(dmpz)₂(BF₄)₂ (starting material). Although the analytical data are in excellent agreement with a bulk dmpz/mpz ratio of 4/2, the presence of some starting material cannot be completely excluded. The presence of some [Cu₂F₂(dmpz)₂(mpz)]²⁺ ions also cannot be excluded.

Model 1 was investigated via a series of refinements involving two tautomeric rings with occupancies totaling 1. Initially, the geometries of these tautomeric rings were constrained upon the mean geometry of the dmpz rings; then the slack constraints were dropped and the positional parameters of neighboring atoms belonging to different tautomers were coupled. However, the tautomeric rings obtained overlapped almost completely, and the values of the residuals ($R = 0.043$, $R_w = 0.066$) were higher than in the second model described below. This fact, together with the higher number of parameters, implies that the tautomeric model is not the best description of the structure.

Model 2 was more satisfactory. The atom attached to C(13) was partly introduced as carbon C(17) (20%) and partly as hydrogen H(13) (80%). With use of slack constraints C(13)-H(13) = 0.96 Å ($\sigma = 0.01 \text{ \AA}$) and C(13)-C(17) = 1.530 Å ($\sigma = 0.005 \text{ \AA}$) the positions and occupancies of C(17) and H(13) were refined together with the parameters of all other atoms (the isotropic thermal parameters of C(17) and H(13) were fixed at 8 Å²). At the final stage the occupancies of C(17) and H(13) were 39 and 61% ($\sigma = 1\%$), respectively. A final difference Fourier synthesis showed a few residual peaks near the BF₄⁻ anion (indicative of some disorder) and two peaks (separated

Table VI. Final Fractional Coordinates ($\times 10^4$) of Non-Hydrogen Atoms in II, with Esd's in Parentheses

atom	<i>x/a</i>	<i>y/b</i>	<i>z/c</i>
Cu	385.5 (5)	1132.4 (4)	4727.5 (3)
F	874 (2)	-13 (2)	5710 (1)
N(11)	1104 (4)	107 (3)	3363 (2)
N(12)	1617 (4)	555 (3)	4040 (2)
C(13)	2944 (5)	452 (5)	4088 (3)
C(14)	3256 (7)	-25 (7)	3438 (5)
C(15)	2059 (6)	-257 (4)	2973 (3)
C(16)	1700 (7)	-785 (5)	2199 (3)
C(17)	4004 (13)	395 (13)	4817 (6)
N(21)	-2315 (4)	2060 (3)	4368 (2)
N(22)	-1215 (4)	2035 (3)	4925 (2)
C(23)	-1536 (5)	2710 (3)	5468 (2)
C(24)	-2834 (6)	3135 (4)	5248 (3)
C(25)	-3305 (5)	2711 (3)	4539 (3)
C(26)	-599 (6)	2896 (5)	6202 (3)
C(27)	-4593 (5)	2885 (5)	4004 (3)
N(31)	2507 (4)	1956 (3)	5926 (2)
N(32)	1749 (3)	2197 (3)	5242 (2)
C(33)	2108 (5)	3229 (3)	5070 (3)
C(34)	3107 (6)	3618 (4)	5646 (3)
C(35)	3328 (5)	2810 (4)	6183 (3)
C(36)	1481 (6)	3759 (4)	4344 (3)
C(37)	4177 (7)	2745 (5)	6940 (3)
B	2712 (6)	-252 (5)	7466 (3)
F(1)	3490 (3)	-58 (3)	6916 (2)
F(2)	3443 (3)	-274 (3)	8172 (2)
F(3)	2086 (5)	-1252 (3)	7259 (2)
F(4)	1709 (3)	545 (3)	7399 (2)

Table VII. Relevant Bond Lengths (Å) and Angles (deg) in II^a with Esd's in Parentheses

Cu-Cu'	2.9962 (9)	Cu-N(12)	1.984 (4)
Cu-F	2.195 (2)	Cu-N(22)	1.997 (3)
Cu-F'	1.901 (2)	Cu-N(32)	1.964 (3)
Cu-F-Cu'	93.73 (8)	F-Cu-F'	86.27 (8)
N(12)-Cu-F	101.1 (1)	N(12)-Cu-F'	86.7 (1)
N(22)-Cu-F	105.9 (1)	N(22)-Cu-F'	87.4 (1)
N(32)-Cu-F	89.2 (1)	N(32)-Cu-F'	175.3 (1)
N(12)-Cu-N(22)	152.0 (2)	N(12)-Cu-N(32)	93.2 (1)
N(22)-Cu-N(32)			94.9 (1)

^a Primed atoms are generated by the center of symmetry.

Table VIII. Hydrogen-Bonding Distances (Å) and Angles (deg) in II,^a with Esd's in Parentheses

N(11)--F'	2.763 (4)	H(11)--F'	2.374 (4)
N(11)--F(4)'	3.003 (5)	H(11)--F(4)'	2.261 (5)
N(21)--F'	2.836 (4)	H(21)--F'	2.441 (4)
N(21)--F(3)'	3.076 (5)	H(21)--F(3)'	2.455 (5)
N(31)--F	2.835 (4)	H(31)--F	2.286 (4)
N(31)--F(1)	3.028 (5)	H(31)--F(1)	2.427 (5)
N(11)-H(11)--F'	112.5 (1)	N(21)-H(21)--F(3)'	147.7 (1)
N(11)-H(11)--F(4)'	161.4 (1)	N(31)-H(31)--F	134.9 (1)
N(21)-H(21)--F'	117.3 (1)	N(31)-H(31)--F(1)	142.9 (1)

^a Very weak hydrogen bonds are omitted. Primed atoms are generated by the symmetry operation $-x, -y, 1-z$.

by 1.95 Å) far from the dimeric Cu₂F₂ unit, for which we could find no interpretation. The final values of the residuals are $R = 0.035$ and $R_w = 0.047$ (R and R_w defined as above) for the 2258 significant reflections used in the refinement. Final fractional coordinates of non-hydrogen atoms are listed in Table VI, while Table VII summarizes the most relevant interatomic distances and angles. Hydrogen-bonding information is given in Table VIII. Additional information (see "I") is given in the supplementary material.

Results and Discussion

Description of I. The numbering scheme of the cation of I is shown in Figure 1. Hydrogen atoms are omitted for clarity. The molecules of I are dimeric, consisting of two CuF(tmpz)₃(BF₄) units related by an inversion center. These

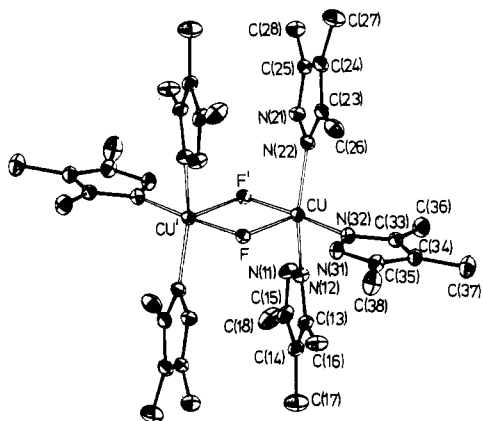


Figure 1. ORTEP drawing (15% probability ellipsoids) of the $[\text{Cu}_2\text{F}_2(\text{tmpz})_6]^{2+}$ cation in I, together with the numbering system used.

units are connected by two asymmetric fluoro bridges, with Cu–F bond lengths of 1.911 (2) and 2.183 (2) Å, respectively. The coordination geometry of the copper atom is square-based pyramidal; the apical position is occupied by the fluorine atom with the longest Cu–F bond length (2.183 Å), while the square base consists of a second fluorine atom (Cu–F = 1.911 Å) and three coordinating nitrogen atoms of the tmpz ligands (Cu–N(12) = 2.013 (3) Å, Cu–N(22) = 2.009 (3) Å, Cu–N(32) = 1.965 (3) Å). The copper atom is at a distance of 0.184 (1) Å from the least-squares plane through the corners of the square base; the corner atoms are separated from this plane by 0.250 (1)–0.308 (1) Å. The ring systems of the ligands are planar, and the maximal distance of the atoms to the least-squares planes is less than 0.006 (2) Å. Pyrazole ring 3 (coordinated at N(32)) is almost parallel to the central Cu_2F_2 plane (dihedral angle 6.1 (1)°), while the other two rings are almost perpendicular to the Cu_2F_2 plane (angle with ring 1 88.8 (1)° and with ring 2 80.1 (1)°). Rings 1 and 2 are almost parallel (dihedral angle 8.7 (2)°) and are at angles of 36.1 (1) and 35.1 (1)°, respectively, with the equatorial Cu–F' bond. The BF_4^- anion was observed to be present in at least two orientations, represented by {B, F(1A), F(2A), F(3A), F(4A)} and {B, F(1B), F(2B), F(3B), F(4B)}. Refinement of the parameters belonging to these orientations resulted in a ratio A/B = 27/73 ($\sigma = 1$); nevertheless the thermal parameters of the fluorine atoms are still high, which implies that additional orientations may be present. Hydrogen-bonding interactions play an important part in stabilizing the structure, a well-known phenomenon in fluorine-containing coordination compounds.^{4–7} In this case the N–H atoms of the substituted pyrazole ligands are involved in asymmetric, trifurcated hydrogen-bonding interactions with one fluorine atom of the Cu–F–Cu bridge and two fluorine atoms of a BF_4^- anion, as is shown in Table V. From this table it is evident that the bridging fluorine atoms are bonded more strongly than the BF_4^- fluorine atoms.

Description of II. The numbering scheme of the cation of II is shown in Figure 2. The molecules of II consist of two $\text{Cu}(\text{mpz})(\text{dmpz})_2$ units connected by two asymmetric fluoro bridges, with Cu–F bond lengths of 1.901 (2) and 2.195 (2) Å, respectively. The coordination geometry of the copper atom is square-based pyramidal, as in I, with the longest Cu–F bond length again involving the fluorine atom in the apical position. All Cu–N distances in II are near 2.0 Å, as in I. The copper atom in II is at a distance of 0.195 (2) Å from the least-squares plane through the corners of the square base. The distances of the corner atoms to this plane vary from 0.248 (1) to 0.293 (2) Å. The ring systems of the ligands are planar, considering that the maximal distance of any of the ring atoms to the least-squares plane is less than 0.008 (3) Å. One dmpz ring

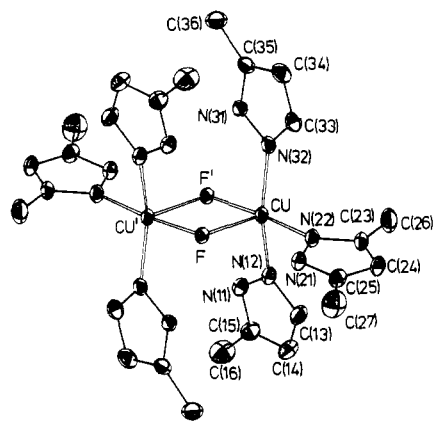


Figure 2. ORTEP drawing (15% probability ellipsoids) of the $[\text{Cu}_2\text{F}_2(\text{mpz})_2(\text{dmpz})_4]^{2+}$ cation in II and the atomic numbering system used.

Table IX. Relevant Distances (Å) and Angles (deg) in Three Very Similar Fluoride-Bridged Copper(II) Dimers, with Esd's in Parentheses

	I	II	III ^a
Distances ^b			
Cu–Cu'	3.0141 (8)	2.9962 (9)	3.131 (3)
Cu–F	2.183 (2)	2.195 (2)	2.258 (2)
Cu–F'	1.911 (2)	1.901 (2)	1.904 (2)
Cu–N	2.013 (3)	1.984 (4)	1.973 (4)
	2.009 (3)	1.997 (3)	1.977 (2)
	1.965 (3)	1.964 (3)	1.978 (3)
Angles ^{b,c}			
Cu–F–Cu'	94.59 (7)	93.73 (8)	97.19 (8)
N _t –Cu–N _t	151.6 (1)	152.0 (2)	159.9 (1)
(Cu–F')–(pz) _t	36.1	31.2 ^d	2.6 ^d
	35.1	40.5 ^e	6.5 ^d
(Cu ₂ F ₂)–(pz)	6.1	3.0	6.0
(Cu ₂ F ₂)–(pz) _⊥	88.8	77.7	83.5
	80.1	97.2	92.9

^a Values are taken from ref 5. ^b Primed atoms are generated by the center of symmetry. ^c Key: t = trans; (Cu–F') = Cu–F' vector; (pz) = substituted pyrazole ring; (Cu₂F₂) = central plane through Cu, Cu', F, and F'. ^d (pz)_t = mpz. ^e (pz)_t = dmpz.

(coordinated at N(32)) is almost parallel to the Cu_2F_2 unit (dihedral angle 3.0 (2)°); the other dmpz ring and the mpz ring are almost perpendicular to it (dihedral angles of 77.7 (1) and 97.2 (2)°, respectively). The dihedral angle between the last two rings is 22.0 (2)°, while the angles with the equatorial Cu–F' bond are 31.2 (2)° (for the mpz ring) and 40.5 (1)° (for the dmpz ring). Fluorine–hydrogen interactions are also quite important in this structure. All N–H atoms of the substituted pyrazole ligands are involved in asymmetric trifurcated hydrogen bond involving one bridging fluorine atom and two fluorine atoms of a BF_4^- anion (Table VIII).

Comparison of Structures. Table IX summarizes relevant distances and angles in three very similar fluoride-bridged copper(II) dimers (I = $[\text{Cu}_2\text{F}_2(\text{tmpz})_6](\text{BF}_4)_2$; II = $[\text{Cu}_2\text{F}_2(\text{dmpz})_4(\text{mpz})_2](\text{BF}_4)_2$; III = $[\text{Cu}_2\text{F}_2(\text{dmpz})_2(\text{mpz})_4](\text{BF}_4)_2$). In all three compounds the copper atom is in a square-based pyramidal geometry. An ORTEP drawing of the cation of III is shown in Figure 3. The Cu–Cu' distances increase in the order II < I < III as is the case with the Cu–F–Cu' angles. The large Cu–Cu' distance in III will be mainly due to an increased Cu–F(apical) distance in III compared to the corresponding distance in the other two compounds. The introduction of extra methyl groups in the pyrazole ligands appears to increase with mean Cu–N(pyrazole) distance: III (2 mpz and 1 dmpz per Cu) < II (1 mpz and 2 dmpz per Cu) < I (3 tmpz per Cu). In all three structures one substituted pyrazole ring is almost parallel to the central Cu_2F_2 plane and two other

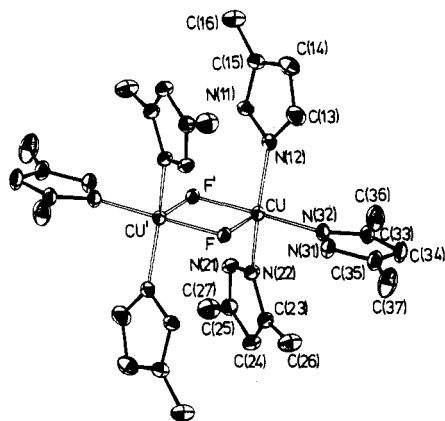


Figure 3. ORTEP drawing of the $[\text{Cu}_2\text{F}_2(\text{mpz})_2(\text{dmpz})_2]^{2+}$ cation in III, redrawn with 15% probability ellipsoids by using the parameters of Ten Hoedt et al.⁵

substituted pyrazole ligands are approximately perpendicular to this plane (angles varying from 77 to 97°). A comparison of the angles between the equatorial Cu–F bond and the two trans ligands (with respect to the Cu atom) shows a remarkable difference: in III the trans ligands (mpz rings) are parallel to the Cu–F bond; in the other two structures there is a twist of 30–40° from this parallel situation. Another difference concerns the nature of the hydrogen-bonding interactions: in both I and II each N–H proton is involved in trifurcated hydrogen bonds (through disordered), while in III the mpz N–H protons interact with only two fluorine atoms (bifurcated hydrogen bonds).

Structurally closely related to I, II, and III is the recently reported¹¹ dimeric compound $\text{Cu}_2(\text{N-MeIm})_4(\text{OAc})_4$ (N-MeIm = N-methylimidazole), containing Cu(II) in square-based pyramidal geometry; in the last compound bridging also occurs in an asymmetrical fashion, but now by monoatomic acetate bridges instead of fluorine atoms. One acetate oxygen is in the apical position (Cu–O = 2.424 (1) Å), while an oxygen atom of another bridging acetate anion (Cu–O = 1.986 (1) Å) is at one of the equatorial positions of the square base. The other three equatorial positions are occupied by two nitrogen atoms of coordinated 1-methylimidazole ligands (Cu–N distances 1.996 (1) and 1.994 (1) Å) and by one oxygen atom of a (third) acetate anion (Cu–O = 1.956 (1) Å).

Spectroscopic and Magnetic Properties. The IR spectra of I, II, and III are very similar in the far-IR region, showing a strong band at about 445 cm^{-1} . Comparison with other copper(II) pyrazole compounds¹² and metal–fluoride compounds⁶ show that this band can be assigned to a Cu–F stretching vibration. The differences in the Cu–F(short) distances (Table IX) are too small to result in different Cu–F stretching vibrations.

The ligand field spectra of all three compounds show a maximum at about $14.0 \times 10^3 \text{ cm}^{-1}$, with a weak shoulder at about $10 \times 10^3 \text{ cm}^{-1}$. These bands are in agreement with the square-pyramidal coordination for the Cu(II) ions.¹³ The bands are too broad to detect possible rhombic splitting (expected because fluoride and pyrazole possess different positions in the spectrochemical series).

Because the Cu–Cu distances in the compounds are rather short, one might expect magnetic exchange interaction between the copper ions. A sensitive method to study such interactions is the determination of the magnetic susceptibility as a function

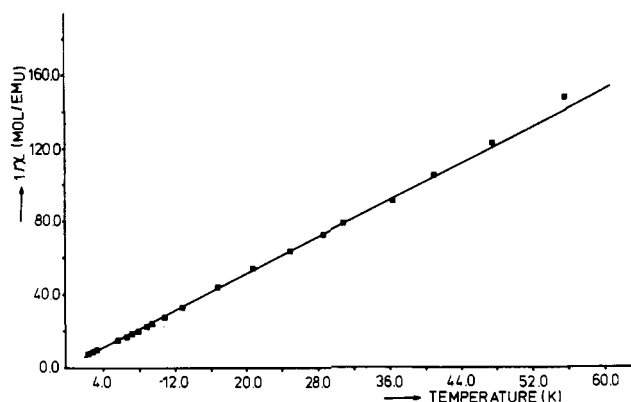


Figure 4. Plot of the reciprocal susceptibility vs. temperature of $[\text{Cu}_2\text{F}_2(\text{mpz})_2(\text{dmpz})_4](\text{BF}_4)_2$ (II). The line drawn was calculated with $\mu = 1.80 \mu_B$ and $\theta = 0.0 \pm 0.2 \text{ K}$.

of temperature.¹⁴ However, magnetic susceptibility measurements down to 2 K of compounds I, II, and III did not show any indication of magnetic exchange. A plot of the reciprocal susceptibility for one of the compounds is given in Figure 4. The behavior is essentially according to the Curie law (the value of θ is $0.0 \pm 0.2 \text{ K}$). Consequently, $|J|$, the exchange parameter determining the singlet–triplet splitting, cannot be larger than 0.4 cm^{-1} .

Another sensitive tool for the study of magnetic interaction in copper dimers is EPR spectroscopy. When two $S = 1/2$ systems are coupled, an EPR spectrum typical of a triplet is usually observed.^{15,16} A large variety of copper dimers is known to show this behavior. Typical indications of triplet spectra are the presence of g values below 2.0, hyperfine interactions with two copper nuclei (resulting in seven lines rather than four), and so-called half-field transitions at about $g = 4.3$ ($\Delta m_S = 2$ transitions).^{15–17}

All three compounds have spectra showing this behavior at both X-band and Q-band frequencies, at temperatures varying from 4 to 300 K. In many cases the triplet spectra allow accurate determination of g values and zero-field splitting parameters. Our spectra, unfortunately, allow only approximate determinations of the zero-field splitting. The results yield $|D| = 0.06\text{--}0.10 \text{ cm}^{-1}$. This behavior is caused by either or both of the following factors: (i) the singlet–triplet splitting is of the same order as D , sometimes resulting in additional singlet–triplet transitions in the EPR spectrum;¹⁸ (ii) the g tensor and the D tensor in these low-symmetry compounds are not necessarily collinear. We plan to study this problem later, using single-crystal EPR spectra as a function of temperature.

In analyzing the origins of the weak overall magnetic exchange coupling, as observed by the magnetic susceptibility, we can exclude the possibility of interdimer exchange, since all three copper compounds have interdimer Cu–Cu distances larger than 9 Å.

Concluding Remarks

The results of the present investigation have shown that interesting new classes of fluoride-bridged copper compounds can be prepared by both controlled-decomposition reactions of tetrafluoroborates in the presence of organic ligands and by ligand-exchange procedures using initially formed copper dimers.

(11) Boukari, P. Y.; Busnot, A.; Busnot, F.; Leclaire, A.; Bernard, M. A. *Acta Crystallogr., Sect. B: Struct. Crystallogr. Cryst. Chem.* **1982**, *B38*, 2458–2461.
 (12) Reedijk, J. *Recl. Trav. Chim. Pays-Bas* **1970**, *89*, 605–618.
 (13) Hathaway, B. J.; Billing, D. E. *Coord. Chem. Rev.* **1970**, *5*, 143–207.

(14) Carlin, R. L.; Van Duijneveldt, A. J. "Magnetic Properties of Transition Metal Compounds"; Springer-Verlag: New York, 1977.
 (15) Wasserman, E.; Snyder, L. C.; Yager, W. A. *J. Chem. Phys.* **1964**, *41*, 1763–1772.
 (16) Reedijk, J.; Knetsch, D.; Nieuwenhuys, B. *Inorg. Chim. Acta* **1971**, *5*, 568–572.
 (17) Chasteen, N. D.; Belford, R. L. *Inorg. Chem.* **1970**, *9*, 169–175.
 (18) Duggan, D. M.; Hendrickson, D. N. *Inorg. Chem.* **1974**, *13*, 2929–2940.

The present and previous⁶ results indicate that the species [(ligand)₃CuF₂Cu(ligand)₃]²⁺ seems to occur quite generally and that stabilization in the solid state by hydrogen-bonding interactions is significant. The copper dimers studied so far show a very weak magnetic exchange interaction, which is likely to be intramolecular. The weak coupling between the copper(II) ions can be understood on the basis of recent results of Kahn¹⁹ and the fact that the square-pyramidal copper coordination geometry results in $d_{x^2-y^2}$ as the magnetic orbitals. With use of this model a co-square-planar geometry for the dimeric unit [L₂CuF₂CuL₂] would result in a significant antiferromagnetic interaction. Such systems are being studied.

(19) Julve, M.; Verdager, M.; Kahn, O.; Gleizes, A.; Philoche-Levisalles, M. *Inorg. Chem.* 1983, 22, 368-370.

Acknowledgment. The authors are indebted to Dr. H. B. Broer-Braam, Prof. Dr. W. J. A. Maaskant, and Dr. G. C. Verschoor for helpful discussions. Thanks are also due to F. B. Hulsbergen and W. Vreugdenhil (all from the State University of Leiden) for their contributions in the early stages of this research. The investigation was supported by the Netherlands Foundation for Chemical Research (SON) with financial aid from the Netherlands Organization for the Advancement of Pure Research (ZWO).

Registry No. I, 87861-49-2; II, 87861-51-6; [CuF₂(dmpz)₆](BF₄)₂, 76171-85-2; Cu(BF₄)₂, 38465-60-0.

Supplementary Material Available: Tables of thermal parameters, hydrogen parameters, least-squares planes, and observed and calculated structure factors (26 pages). Ordering information is given on any current masthead page.

Contribution from The Procter & Gamble Company, Miami Valley Laboratories, Cincinnati, Ohio 45247

Synthesis and Crystal Structure of Dibromotetrakis(dimethyl sulfoxide)ruthenium(II). Structural Implications for O₂ Oxidation Catalysis

JOEL D. OLIVER* and DENNIS P. RILEY

Received April 26, 1983

In an effort to elucidate the mechanism of the oxygen oxidations of sulfides to sulfoxides with the RuX₂(Me₂SO)₄ (X = Cl or Br) catalysts, we determined the crystal structure of the RuBr₂(Me₂SO)₄ catalyst. Unlike the chloro-based catalyst that possesses a cis geometry and O- and S-bonded Me₂SO ligands, RuBr₂(Me₂SO)₄ has a trans structure with all S-bonded Me₂SO ligands. The molecule has crystallographic 4/*m* (*D*_{4h}) symmetry with the Ru, S, and O atoms lying on the crystallographic mirror plane. The Ru-S bond lengths exhibit a trans influence. Principal metrical details are Ru-Br = 2.540 (1) Å, Ru-S = 2.360 (1) Å, S-O = 1.484 (3) Å, S-C = 1.789 (3) Å, Ru-S-O = 112.5 (1)°, Ru-S-C = 116.0 (1)°, C-S-O = 105.7 (1)°, and C-S-C' = 99.6 (2)°. Crystals of the complex are tetragonal, of space group *I4/m* (No. 87), with *a* = 9.181 (2) Å, *c* = 11.121 (2) Å, and *Z* = 2. Least-squares refinement of the structure has resulted in *R* = 0.018 and *R*_w = 0.025 based on 403 unique reflections with $|F| \geq 5\sigma(|F_o|)$.

Introduction

Our interest in Ru(II) complexes of the type RuX₂(Me₂SO)₄ stems from our observation that such complexes act as excellent, selective sulfide oxidation catalysts using molecular oxygen.² A puzzling aspect of our work with these catalysts is that the RuBr₂(Me₂SO)₄ complex is a much more active catalyst than the RuCl₂(Me₂SO)₄ complex.³ The possible structural origin of such reactivity differences prompted us to determine the solid-state structure of the RuBr₂(Me₂SO)₄ catalyst.

The structure of the RuCl₂(Me₂SO)₄ complex (**1**) has been determined previously by X-ray diffraction techniques⁴ and was shown to have a cis arrangement of the chloride ligands with three S-bonded Me₂SO ligands and one O-bonded Me₂SO mutually cis to each chloro ligand. Attempts to determine the structure of RuBr₂(Me₂SO)₄ unambiguously using IR, ¹H NMR, and UV-vis spectra did not provide a conclusive structural assignment. Thus, an X-ray structure analysis of the complex was initiated. The results of this X-ray study are presented herein.

Experimental Section

Materials. The RuBr₂(Me₂SO)₄ complex (**2**) was prepared by the method of James et al.¹ Crystals of **2** suitable for the X-ray diffraction study were obtained by dissolving under an Ar atmosphere 0.5 g of the pale yellow crude RuBr₂(Me₂SO)₄ in 100 mL of hot (110 °C) 70% toluene-30% Me₂SO solvent mixture. Filtration of this hot

solution followed by slow cooling at 20 °C gave orange-red crystals after 2 days. These crystals were collected by filtration to give 0.21 g of **2**. Storage of the filtrate at -40 °C for an additional 2 weeks gave a second crystalline crop of 0.23 g of **2**. Both crops were shown to be structurally identical with the starting material by comparison of their IR and UV-vis spectra. Electronic spectrum (CHCl₃) [λ_{\max} , cm⁻¹ (ϵ): 21 380 (207), 32 050 (sh), 37 600 (2740)]. Selected absorptions in the infrared spectrum [cm⁻¹ (assignment,⁵ intensity)]: 1300 (δ (d)_{CH}, s), 1289 (δ (d)_{CH}, s), 1082 (ν _{SO}, s), 1028 (CH rock, s), 720 (ν _{CS}, s), 674 (ν _{CS}, s) 520 (broad and intense), 479 (ν _{RuS}, s), 431, 390 (δ _{CSO}, s).

Physical Measurements. ¹H NMR spectra were recorded in CDCl₃ solution at 270 MHz on a JEOL FX-270 spectrometer. Solid-state infrared spectra were recorded as Nujol mulls between CsBr windows on Perkin-Elmer Model 298 and 621 spectrophotometers. Electronic spectra were recorded in the UV-vis regions on a Beckman DU-7 spectrophotometer as chloroform solutions in stoppered quartz cells.

Crystallographic Study of 2. The crystals changed color from orange-red to yellow during storage prior to collecting the single-crystal diffraction data. The solution (CHCl₃) UV-vis spectrum and the solid-state IR spectrum of the yellow crystals were identical with those of the orange crystals. The source of this color change remains unclear (vide infra). A yellow, octahedral-shaped crystal was mounted on a glass fiber and transferred to a Syntex P₂ diffractometer equipped with a graphite monochromator and a Mo-target X-ray tube. The crystal data and details of the data collection are presented in Table I.

The systematic absences listed in Table I are consistent with the space group choice of *I4*, $\bar{I}4$, or *I4/m* for the crystals. The crystal structure was solved intuitively by placing the Ru atom at a 4/*m* site and placing the Br atom along the 4-fold axis 2.5 Å above the Ru atom in space group *I4/m*. A difference map revealed the locations

(1) James, B. R.; Ochiai, E.; Rempel, G. I. *Inorg. Nucl. Chem. Lett.* 1971, 7, 781.

(2) Riley, D. P. *Inorg. Chem.* 1983, 22, 1965.

(3) Ledlie, M. A.; Allum, K. G.; Howell, I. V.; Pitkethly, R. C. *J. Chem. Soc., Perkin Trans. 1* 1976, 1734-8.

(4) Mercer, A.; Trotter, J. J. *J. Chem. Soc., Dalton Trans.* 1975, 2480-3.

(5) Evans, I. P.; Spencer, A.; Wilkinson, G. *J. Chem. Soc., Dalton Trans.* 1973, 204.